



PTPMT1 inhibition induces apoptosis and growth arrest of human SCLC cells by disrupting mitochondrial metabolism

Xiang Liu^{1#}, Yang Sun^{2#}, Chuancheng Gao³, Huiyan Sun⁴, Fang Tian^{5,6}, Fengjun Xiao^{3*}, Qinqin Xu^{5*}

¹Emergency Department, Qinghai Provincial People's Hospital, Xining, China; ²School of Basic Medicine, Qingdao University, Qingdao, China; ³Beijing Institute of Radiation Medicine, Beijing, China; ⁴Medical Research Institute, Hebei Yanda Hospital, Sanhe, China; ⁵Department of Medical Oncology, Qinghai Provincial People's Hospital, Xining, China; ⁶Qinghai University, Xining, China

Contributions: (I) Conception and design: X Liu, Y Sun, C Gao, F Xiao; (II) Administrative support: Q Xu, F Xiao; (III) Provision of study materials or patients: Y Sun, C Gao; (IV) Collection and assembly of data: Y Sun, H Sun, F Tian, Q Xu; (V) Data analysis and interpretation: X Liu, Y Sun, C Gao; (VI) Manuscript writing: All authors; (VII) Final approval of manuscript: All authors.

[#]These authors contribute equally to this work.

^{*}These authors contributed equally to this work.

Correspondence to: Qinqin Xu, MD. Department of Medical Oncology, Qinghai Provincial People's Hospital, Gonghe Road, Xining 810001, China. Email: 13997075521@163.com; Fengjun Xiao, PhD. Beijing Institute of Radiation Medicine, 27 Taiping Road, Beijing 100850, China. Email: xiaofjun@sina.com.

Background: Many cancer cells exhibit aberrant metabolic reprogramming through abnormal mitochondrial respiration. Protein tyrosine phosphatase mitochondrial 1 (PTPMT1) is a protein tyrosine phosphatase localized to the mitochondria and linked to mitochondrial respiration. However, the expression and role of PTPMT1 in regulating the biological characteristics of small cell lung cancer (SCLC) has not yet been explored. The aim of this study was to evaluate the role of PTPMT1 on SCLC cell survival and mitochondrial function.

Methods: SCLC and adjacent normal tissues were obtained from surgery. The expression level of PTPMT1 in the SCLC tissues and cell lines was determined by immunohistochemical staining, western blot, and quantitative real-time polymerase chain reaction (qRT-PCR). PTPMT1 knockdown was induced by lentivirus-mediated short-hairpin RNA (shRNA) transduction and PTPMT1 inhibition (alexidine dihydrochloride). The biological characteristics of the cells were measured by cell counting kit 8 (CCK-8), colony formation assay, and cell migration assay. The mitochondrial function of the cells was measured by 5,5',6,6'-tetrachloro-1,1',3,3'-tetraethylbenzimidazolylcarbocyanine iodide (JC-1) staining. The H69 cells were treated with alexidine dihydrochloride, after which transcriptome sequencing and an untargeted metabolomic analysis were performed. The transcriptome differentially expressed genes were measured by qRT-PCR.

Results: PTPMT1 was upregulated in the SCLC tissues compared to the adjacent normal tissues. PTPMT1 inhibition by lentiviral shRNA transduction or specific inhibition resulted in significant growth arrest and apoptosis. The transcriptome sequencing analysis revealed that pathways related to the respiration chain and mitochondrial member protein were disrupted. Several mitochondrial metabolism-related genes, such as *FGF21*, *GDF-15*, *APLN*, and *MT-DN6*, were dysregulated. Further, PTPMT1 inhibition was found to downregulate Glut expression and disturb mitochondrial function.

Conclusions: PTPMT1 was shown to play a critical role in the survival and growth of SCLC cells, and may become a potential therapeutic target.

Keywords: Small cell lung cancer (SCLC); protein tyrosine phosphatase mitochondrial 1 (PTPMT1); proliferation; apoptosis; mitochondrial metabolism

Submitted Nov 27, 2024. Accepted for publication Dec 19, 2024. Published online Dec 27, 2024.

doi: 10.21037/tcr-2024-2379

View this article at: <https://dx.doi.org/10.21037/tcr-2024-2379>

Introduction

Lung cancer is a leading cause of cancer-related death worldwide (1). The two main types of lung cancer are small cell lung cancer (SCLC) and non-small cell lung cancer (NSCLC). NSCLC can be further divided into three histological subtypes: adenocarcinoma, squamous carcinoma, and large cell carcinoma. SCLC is an aggressive growing cancer with high incidences of tumor relapse, metastasis, and chemotherapy resistance (2-4). Currently, SCLC accounts for 15–20% of all lung cancer cases (5). Its 5-year overall survival rate is about 6–31% and associated with the treatment (6,7). The mechanisms leading to chemoresistance are not yet known, and patient prognosis is poor in SCLC (8,9). Thus, novel targets for the molecular pathological diagnosis and treatment of SCLC need to be identified.

Aberrant mitochondrial metabolism is considered the major biological characteristic of cancer cells (10), which offers key metabolites and generates oncometabolites for cancer invasion and metastasis (11). The targeting of mitochondrial metabolism represents a promising approach for the treatment of cancer (12). Protein tyrosine phosphatase mitochondrial 1 (PTPMT1) is a dual-specificity protein tyrosine phosphatase localized to the mitochondrion (13,14) and is linked to glucose metabolism

via succinate dehydrogenase phosphorylation (15). It regulates mitochondrial oxidation and plays important roles in postnatal cerebellar development and hematopoietic stem cell (HSC) expansion (16,17). Research has shown that PTPMT1 deficiency in mice leads to fatal changes in HSCs via metabolism reprogramming (18). PTPMT1 deletion impairs stem-like cluster of differentiation CD8⁺ T cell maintenance and accelerates cell exhaustion/dysfunction (19). A mechanism study has shown that PTPMT1 interacts with micropeptide in mitochondria (MPM) and is associated with the serine/threonine protein kinase B (AKT) pathway (20). There are two PTPMT1 isoforms in cells, and PTPMT1 alternative splicing has been shown to be associated with the radiotherapy sensitivity of lung cancer cells (21). PTPMT1 is essential for the survival of cancer cells. Research has shown that the inhibition of PTPMT1 causes a metabolic crisis and induces cell death in cervical cancer Hela cells (22). Additionally, PTPMT1 was identified as an effector for hypoxic survival and cancer development in hepatocellular carcinoma (23). Further, growing evidence suggests that PTPMT1 is aberrantly expressed and plays important roles in the progress of several types of cancer (24,25). However, it remains unclear whether PTPMT1 and its molecular mechanisms are involved in the pathological progression of SCLC. In the present study, we examined PTPMT1 expression in SCLC patient samples, investigated the roles of PTPMT1 in lung cancer cell proliferation and apoptosis, and compared differential genes and metabolites after inhibiting PTPMT1. We present this article in accordance with the MDAR reporting checklist (available at <https://tc.amegroups.com/article/view/10.21037/tcr-2024-2379/rc>).

Highlight box

Key findings

- Protein tyrosine phosphatase mitochondrial 1 (PTPMT1) might provide a novel therapeutic approach in the treatment of small cell lung cancer (SCLC).
- PTPMT1 is aberrantly expressed in SCLC tumor samples.
- Targeting PTPMT1 suppresses the growth and induces the apoptosis of SCLC cells.
- PTPMT1 inhibition influences the Glut expression and disturbs the mitochondrial function of SCLC cells.

What is known, and what is new?

- PTPMT1 is a critical mitochondrial phosphatase anchored in the mitochondrial inner member, and its dysregulation is linked to the aberrant mitochondrial metabolism of tumor cells.
- We showed that PTPMT1 was aberrantly expressed in SCLC tumor samples. Our functional studies showed the essential role of PTPMT1 in the survival and mitochondrial metabolism of SCLC cells.

What is the implication, and what should change now?

- PTPMT1 could serve as a novel potential diagnostic biomarker and therapeutic target for SCLC.

Methods

Cell culture

NCI-H69 (a human SCLC cell line) was purchased from Procell (Wuhan, China) and cultured in 1640 medium (Gibco, Waltham, MA, USA) supplemented with 10% fetal bovine serum (FBS) (Gibco). A549 (a human NSCLC cell line) was purchased from Procell, and maintained and cultured in Ham's F-12K medium (Procell) supplemented with 10% FBS (Gibco). The PTPMT1 inhibitor (alexidine dihydrochloride) was purchased from Sigma (Germany).

Patient samples

SCLC tissue samples and adjacent normal samples were

Table 1 The forward and reverse sequences of primers used in qRT-PCR

Target	Forward (5'-3')	Reverse (5'-3')
β -actin	CATCCTCACCCCTGAAG TACCC	AGCCTGGATAGCAACGTACATG
PTPMT1	GCACCTTGACACCTGCTTC	GAAATGACAAAAGTCCCATCC
Glut1	GCTCATCCTCCTCCTTCACC	CCAAATCGGCATCTTCTCAT
Glut3	AGCCCACACTTGAGAGGATG	AAGGGAAAGGGACTGAGC
FGF21	ATGGATCGCTCCACTTTGACC	GGGCTTCGGACTGGTAAACAT
LAMP3	ACTACCCCAGCGACTACAAAA	CTAGGGCCGACTGTAACCTCA
GDF15	GACCCTCAGAGTTGCACTCC	GCCTGGTTAGCAGGTCCTC
APLN	GTCTCCTCCATAGATTGGTCTGC	GGAATCATCCAACTACAGCCAG
MT-ND6	CAAACAATGTTCAACCAGTAACCACTAC	ATATACTACAGCGATGGCTATTGAGGA

qRT-PCR, quantitative real-time polymerase chain reaction.

obtained from Qinghai Provincial People's Hospital. The study was conducted in accordance with the Declaration of Helsinki (as revised in 2013). The study was authorized by Human Genetic Resource Administration of China (No. 2021SLCJ2445) and approved by ethics board of Qinghai Provincial People's Hospital (No. 2021-14-1). The informed consent was taken from all the patients.

Immunohistochemistry staining

The SCLC tissues and adjacent normal tissues were embedded in paraffin and cut into slices using a paraffin slicing machine (Leica, Germany). The tissues were dewaxed and then underwent antigen retrieval. The tissues were then blocked with hydrogen peroxide and bovine serum albumin. After blocking, the primary antibody (Novus Biologicals, LLC, CO, USA) was added to the tissues and incubated at 4 °C overnight. After washing the primary antibody, the secondary antibody was added to the tissues and incubated at room temperature for 60 minutes. Next, several steps, including 3,3',4,4'-biphenyltetramine tetrahydrochloride (DAB) chromogenic detection, hematoxylin staining, tissue dehydration, and transparent, were conducted. The tissue slides were photographed by light microscopy (Leica).

Lentivirus-mediated PTPMT1-shRNA transduction

The A549 cells underwent lentivirus-mediated short-hairpin RNA (shRNA) transduction as described previously

(25,26). The lentivirus vector pLKO.1-PTPMT1-shRNA and packaging plasmids psPAX2 and pMD2.G were co-transfected into 293T cells to produce virus supernatant. The virus supernatant was collected, filtered, and concentrated by polyethylene glycol (PEG) according to standard protocols. The titer of the concentrated lentivirus was determined by its infectious efficiency in the human fibrosarcoma HT1080 cells. The H69 and A549 cells were transduced with lentivirus at a multiplicity of infection (MOI) of 10. The knockdown efficiency of the H69 cells was confirmed by western blot and quantitative real-time polymerase chain reaction (qRT-PCR).

qRT-PCR assay

Total RNAs were extracted using TRIzol reagent (Invitrogen Life Technologies, Carlsbad, CA, USA), and the complementary DNA (cDNA) was synthesized using a RevertAidTM cDNA synthesis kit (Thermo Scientific, Wilmington, DE). The SYBR Green I-based qRT-PCR assay was performed using the 7500 detection system (Thermo Scientific). The primers for *PTPMT1*, *Glut1*, *Glut3*, *FGF21*, *LAMP3*, *GDF15*, *APLN*, *MT-ND6* and β -Actin are listed in Table 1. All primers were synthesized by Sangon Biotech (Beijing, China). β -actin was used as an internal control. Gene expression was evaluated by cycle threshold (Ct) values and analyzed using the $2^{-\Delta\Delta C_t}$ method. The messenger RNAs (mRNAs) were quantified, and the relative expression levels of the target genes were determined.

Colony formation assay

The A549 cells were transduced with PTPMT1 shRNA and the control vector, respectively. The transduced cells were cultured in the presence of 1 µg/mL puromycin (MedChemExpress, New Jersey, USA) for 7 days, the number of stained colonies were counted.

Cell migration assay

The A549 cells were incubated in a 6-well plate until the cell density reached 80%. The cells were infected with PTPMT1-shRNA lentivirus and the control vector at a MOI of 10. The cells were then scratched to make the same width among different groups. After incubation for 24 hours, the blank area proportions and cell numbers were counted.

Cell proliferation assay

The cell counting kit 8 (CCK-8) assay was used to detect the proliferation ability of the H69 and A549 cells. At a density of 2×10^4 , the H69 and A549 cells were placed in a 96-well plate and cultured for indicated periods. Next, 10 µL/well of CCK-8 solution (Bimake, Houston, USA) was added to the well, and the proliferation of the H69 and A549 cells was determined by absorbance at a wavelength of 450 nm (Molecular Devices, USA).

Apoptosis assay

The A549 cells were cultured at 37 °C for 48 hours in the presence of PTPMT1 inhibitors. The cells were washed with cold phosphate-buffered saline (PBS) and re-suspended in Annexin-V binding buffer in accordance with the manufacturer's instructions (MultiSciences, Hangzhou, China). The cells were stained by Extracellular phosphatidylserine binding protein V (Annexin V)-allophycocyanin (APC), and apoptosis was detected by flow cytometry (BD FACSCelesta™, BD Biosciences, San Diego, CA, USA).

Western blot

The cells were lysed in Radio Immunoprecipitation Assay (RIPA) buffer (Meilunbio, Dalian, China) containing 1% phenylmethanesulfonyl fluoride and 1% phosphatase

inhibitors. A total of 20 µg of proteins were separated on 12% sodium dodecyl sulfate-polyacrylamide gel electrophoresis gels and transferred to nitrocellulose membranes (Millipore, Germany). The membranes were blocked with 5% non-fat milk in PBS for 1 hour and labeled with primary antibody anti-PTPMT1 (1 µg/mL) (Novus), and then the primary antibody was labeled with goat anti-rabbit IgG H&L (Horseradish peroxidase, HRP) secondary antibody (ZSGB-Bio, Beijing, China), and the membranes were visualized by enhanced chemiluminescence (Pierce Biotechnology, IL, USA).

Measurement of mitochondrial function by JC-1 staining

The H69 cells were transduced with pLKO.1-PTPMT1-shRNA, or the control vector, respectively. After 48 hours, the transduced cells were stained with JC-1 staining solution (BD™ MitoScreen Kit). These cells were incubated for 20 minutes in ice, and fluorescence was detected by flow cytometry (BD FACSCelesta™). Mitochondrial function is represented by the ratio of the average red/green fluorescence intensity.

Transcriptome sequencing

The H69 cells were treated with alexidine dihydrochloride at a concentration of 2 µM for 24 hours. Two H69 cell groups, a control group and an alexidine dihydrochloride group, underwent transcriptome analysis (Biomarker Technologies, Beijing, China). Every group had three biological repeats. A total of 1×10^6 cells were collected using TRIzol reagent (Sigma) in every repeat. After the qualified samples were tested, the library construction was then carried out. The mRNA was enriched by magnetic beads with Oligo (dT) and randomly interrupted by fragmentation buffer. Next, the double-stranded cDNA was synthesized and purified. The cDNA library was then obtained by PCR enrichment. Finally, all the data were sequenced using the Illumina high-throughput sequencing platform and analyzed using bioinformatics approaches. Gene expression level was measured by fragments per kilobase of transcript per million fragments mapped (FPKM). The functional annotation and enrichment analysis of the differentially expressed genes were performed using the Gene Ontology (GO) (<https://www.geneontology.org/>) and Kyoto Encyclopedia of Genes and Genomes (KEGG) (<https://www.genome.jp/kegg/>) databases.

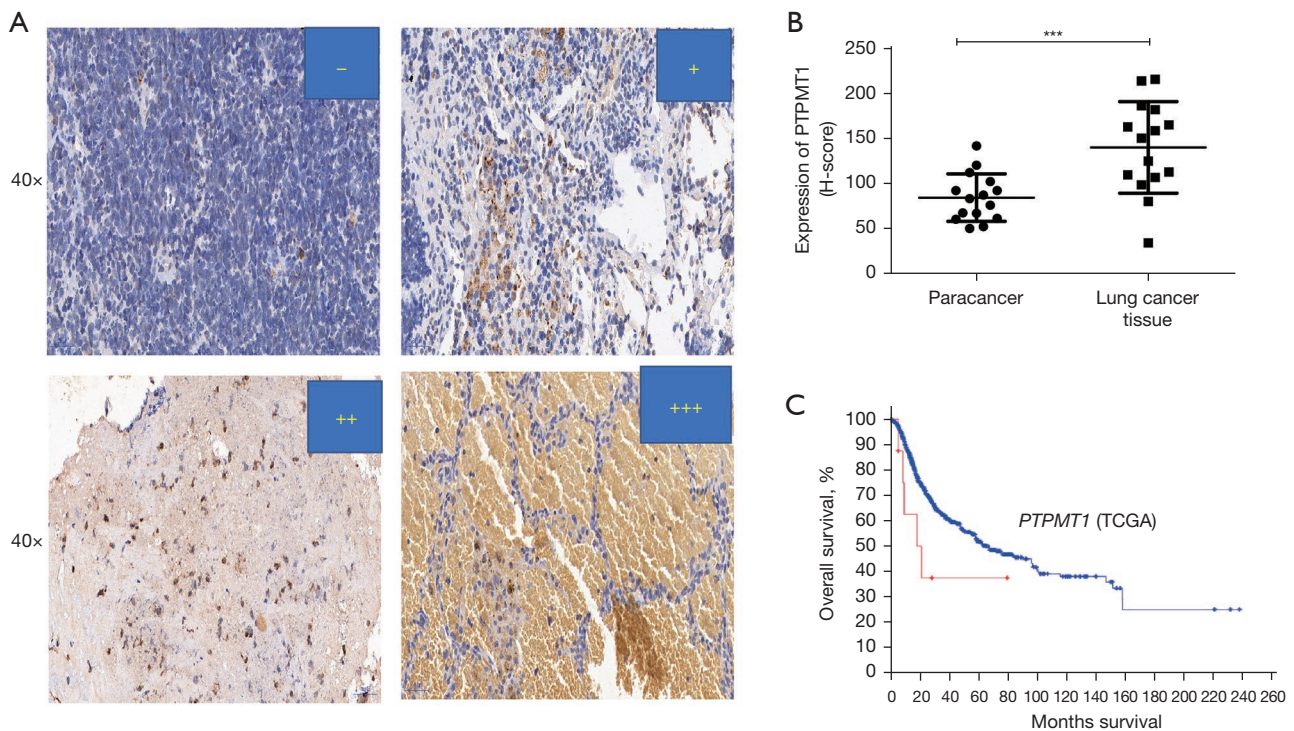


Figure 1 PTPMT1 expression is elevated in SCLC tissues. (A) PTPMT1 expression level was examined by immunostaining. The expression grade of PTPMT1 in human SCLC tissues and their adjacent normal specimens is marked as –, +, ++, and +++ (‘–’: negative; ‘+’: weak intensity; ‘++’: moderate intensity; ‘+++’: strong intensity). (B) PTPMT1 was significantly elevated in human lung cancer tissues. ***, $P < 0.001$, paracancer tissue *vs.* lung cancer tissue. (C) The relationship between PTPMT1 expression and the survival of lung cancer patients. PTPMT1, protein tyrosine phosphatase mitochondrial 1; SCLC, small cell lung cancer; TCGA, The Cancer Genome Atlas.

Untargeted metabolomics

The treatment measures for the H69 cells were the same as those for the transcriptome sequencing. Every group had five biological repeats. The cells were collected by centrifugation and frozen in liquid nitrogen. The metabolomic analyses were conducted by Biomarker Technologies. The analyses were based on the liquid chromatography quadrupole time-of-flight mass spectrometry (LC-QTOF) platform. Metabolite level was determined in the positive or negative ion mode. A cluster analysis of the metabolic pathways was conducted using the KEGG, Human Metabolome (<https://hmdb.ca/>), and LIPID-MAPS (<https://lipidmaps.org/>) databases.

Statistical analysis

The data were analyzed using GraphPad Prism version 9.0 software (CA, USA). The data obtained from the multiple experiments are reported as the mean \pm standard deviation.

The significance levels were tested using the Student’s *t*-test and an analysis of variance. P value < 0.05 was considered statistically significant.

Results

PTPMT1 is aberrantly expressed in SCLC tissues

To elucidate the pathological roles of PTPMT1 in SCLC, the protein levels of PTPMT1 in the SCLC tissues were detected by immunohistochemistry staining. As *Figure 1A, 1B* shows, the PTPMT1 protein level in the SCLC tissues was significantly higher than that in the adjacent normal tissues. The average H-score of the PTPMT1 staining density is shown in *Figure 1B*. Further, the relationship between the overall survival of patients and PTPMT1 expression was analyzed using a comprehensive dataset from The Cancer Genome Atlas (TCGA) (<https://portal.gdc.cancer.gov/>) and the cBioPortal online representation tool (<https://www.cbioportal.org/>). The results showed that PTPMT1

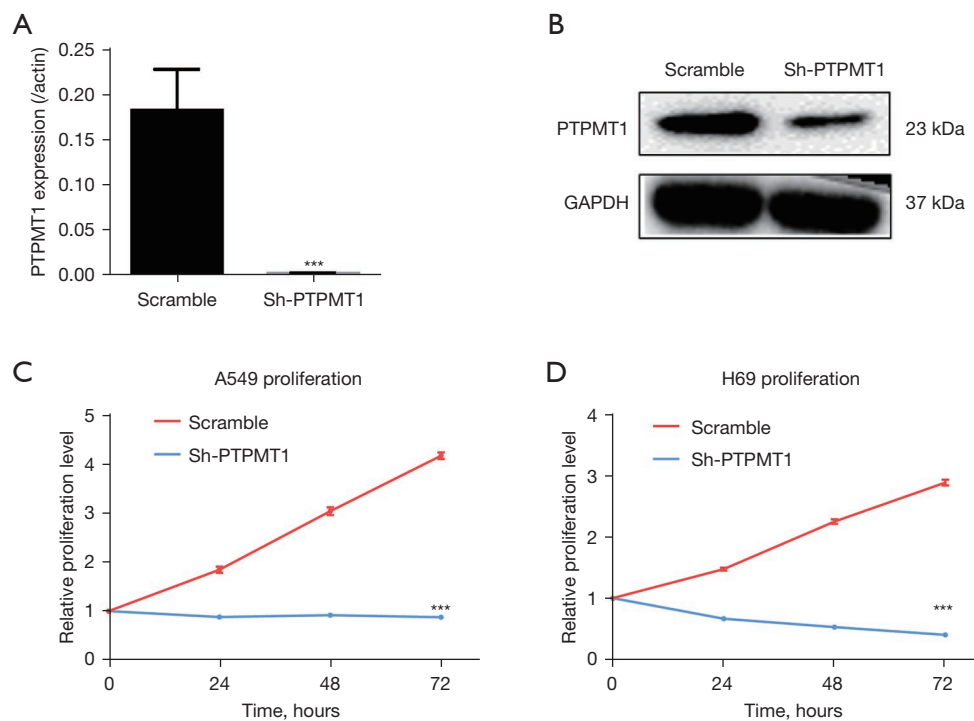


Figure 2 PTPMT1 knockdown reduces cell growth in A549 cells. PTPMT1 mRNA expression (A) and protein level (B) were significantly decreased in PTPMT1-shRNA-transfected cells. (C) CCK-8 assay for cell proliferation of PTPMT1-shRNA-transduced A549. (D) CCK-8 assay for cell proliferation of PTPMT1-shRNA-transduced H69 cells. ***, $P < 0.001$, *vs.* scramble (control). PTPMT1, protein tyrosine phosphatase mitochondrial 1; mRNA, messenger RNA; CCK-8, cell counting kit 8; shRNA, short-hairpin RNA.

overexpression was associated with a lower survival in patients with lung cancer (Figure 1C).

Lentivirus-mediated PTPMT1 knockdown suppresses the growth of H69 and A549 cells

The H69 and A549 cells were transduced with lentivirus-PTPMT1-shRNA or the control vector, respectively. PTPMT1 expression at the mRNA level was confirmed by qRT-PCR. The transduction of PTPMT1-shRNA resulted in significant PTPMT1 silencing in the A549 cells (Figure 2A). Consistent with the qRT-PCR data, the western blot results showed that the PTPMT1 protein level was significantly reduced in the PTPMT1-shRNA transduced cells (Figure 2B). CCK-8 assay was used to examine the proliferation of the PTPMT1-shRNA-transduced A549 and H69 cells. The knockdown of PTPMT1 significantly inhibited growth in both the A549 cells (Figure 2C) and H69 cells (Figure 2D).

PTPMT1 knockdown suppresses colony formation and migration

The inhibitory effect of PTPMT1 silencing on cell growth was further confirmed by the colony forming assay. As Figure 3A,3B shows, the numbers of colonies formed by the PTPMT1-shRNA-transduced A459 cells were significantly lower than those formed by the control group. Further, the scratch assay showed that the migration ability of the PTPMT1-shRNA-transduced A459 cells was significantly reduced (Figure 3C,3D). Thus, PTPMT1 promoted proliferation and migration in the A549 cells.

PTPMT1 knockdown induces the apoptosis of the H69 and A549 cells

Cell apoptosis was examined by Annexin V staining assay. A significant increase in apoptosis was observed in the

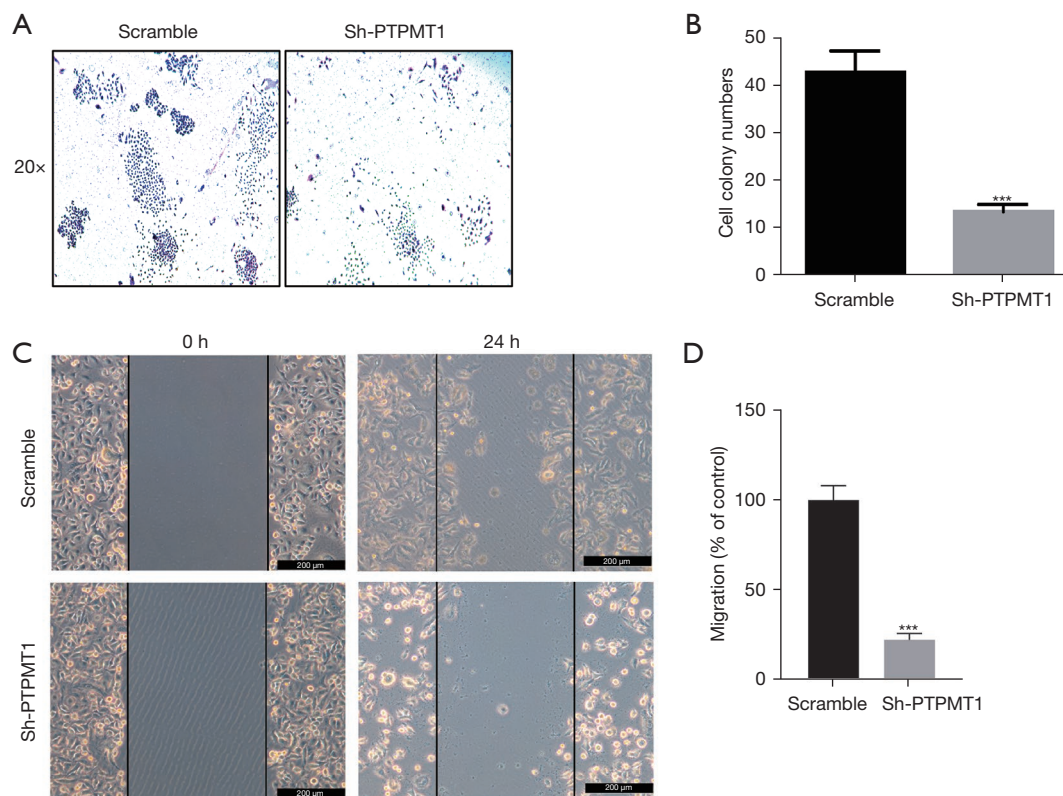


Figure 3 PTPMT1 knockdown inhibits A549 colony formation and migration. (A) Colony formation assay with Giemsa staining for PTPMT1-shRNA-transfected A549 cells. (B) Cell colony numbers for PTPMT1-shRNA-transfected A549 cells. (C) Cell migration by scratch assay for PTPMT1-shRNA-transfected A549 cells. (D) The migration rate of PTPMT1-shRNA transfected A549 cells. ***, $P < 0.001$, sh-PTPMT1 vs. scramble (control). PTPMT1, protein tyrosine phosphatase mitochondrial 1; shRNA, short-hairpin RNA.

PTPMT1-shRNA-transfected cells compared to the control vector-transfected cells (Figure 4A,4B). Thus, the results showed that PTPMT1 knockdown reduced growth and induced apoptosis in the H69 and A549 cells.

PTPMT1 inhibition induces A549 cell death independent of the iron pathway

We further examined the effect of the PTPMT1 inhibitor alexidine dihydrochloride on the viability of the A549 and H69 cells. Alexidine dihydrochloride significantly reduced the viability of the A549 and H69 cells. Ferroptosis is a newly identified type of cell death that is driven by accumulated iron-dependent lipid reactive oxygen species. To determine if the iron was involved in the alexidine dihydrochloride-induced cell death, we observed the reverse effect of Fer-1 on the survival of the A549 and H69 cells treated with the PTPMT1 inhibitor. The pretreatment of

the A549 cells and H69 cells with Fer-1 did not reverse the toxic effect of the alexidine dihydrochloride (Figure 4C,4D). Thus, these results suggest that PTPMT1 inhibition-induced cell death was independent of the iron pathway.

Transcriptome sequencing analysis

A volcano plot was used to show the differences in the expression levels of the genes in the control and alexidine dihydrochloride groups (Figure 5A). The top 10 upregulated and downregulated genes between the two groups were integrated in a heat map (Figure 5B). A GO analysis was conducted to examine the most enriched GO terms across three categories (i.e., biological processes, cellular components, and molecular functions). In terms of the cellular components, the most significant changes were observed in the respiratory chain protein and mitochondria inner membrane. In terms of the biological processes,

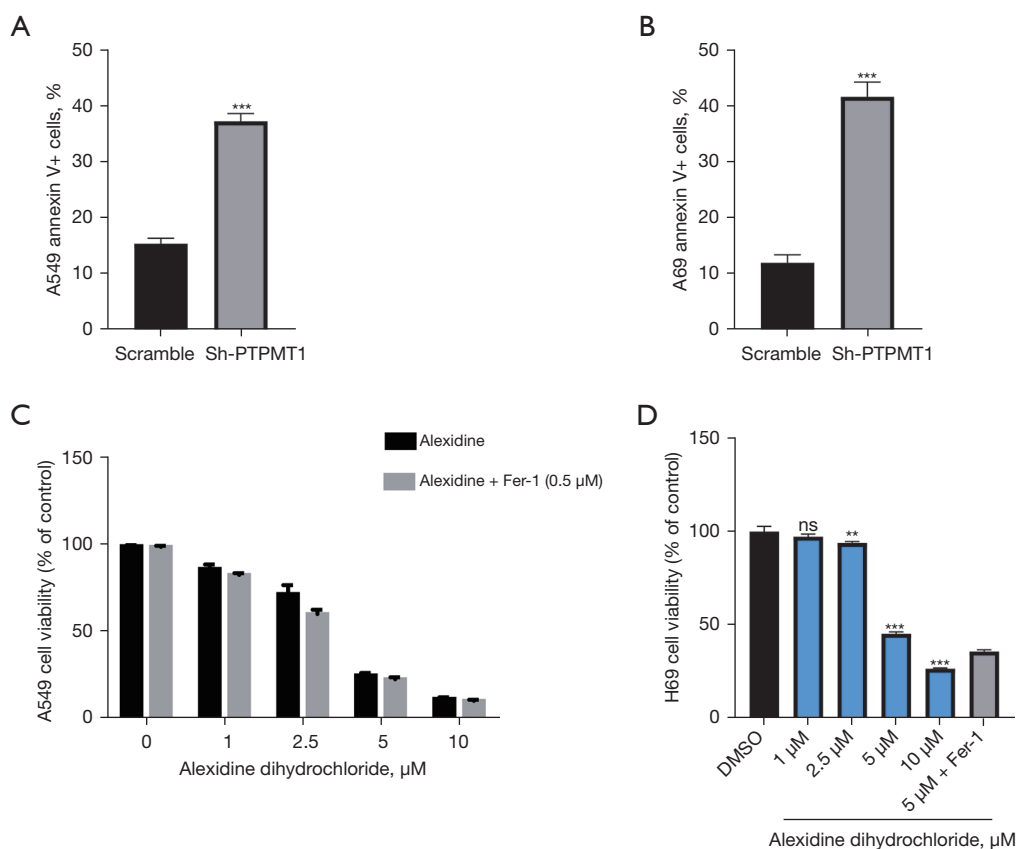


Figure 4 PTPMT1 inhibition induces cell death in A549 cells. (A,B) The percentage of apoptosis in the A549 and H69 cells transduced with PTPMT1-shRNA or control shRNA assessed by annexin-V assay and flow cytometry. ***, $P < 0.0001$, sh-PTPMT1 *vs.* scramble (control). (C) The cell viability of A549 cells treated with alexidine dihydrochloride in the presence of Fer-1. (D) The cell viability of H69 cells treated with alexidine dihydrochloride in the presence of Fer-1. ns, no significance; **, $P < 0.01$, alexidine dihydrochloride 2.5 μM *vs.* control (DMSO); ***, $P < 0.001$, alexidine dihydrochloride 5 μM /10 μM *vs.* control (DMSO). PTPMT1, protein tyrosine phosphatase mitochondrial 1; shRNA, short-hairpin RNA; DMSO, dimethylsulfoxide.

the most significant pathways were related to adenosine-triphosphate (ATP) synthesis coupled electron transport. In terms of the molecular functions, the most significant change was observed in nicotinamide adenine dinucleotide (NADH) dehydrogenase activity (Figure 5C).

Untargeted metabolomics analysis

Volcano plots were used to show the differential metabolites of the alexidine dihydrochloride group relative to the control group (Figure 6A). In total, 75 metabolites were upregulated and 731 were downregulated in the positive ion mode, while 173 were upregulated and 168 were downregulated in the negative ion mode. Figure 6B shows the metabolite classification based on the KEGG functional

annotation. Most metabolites were enriched in carboxylic acids and derivatives, glycerophospholipids, and fatty acyls in both the positive and negative ion modes. Figure 6C shows the differential metabolites enriched by KEGG pathways.

PTPMT1 inhibition downregulates *Glut-1* and *Glut-3* expression, and disturbs mitochondrial function

The expression of significantly changed RNA transcripts, such as *FGF21*, *LAMP3*, *GDF15*, *APLN*, and *MT-ND6*, in the PTPMT1-inhibited cells was further validated by qRT-PCR in the H69 cells (Figure 7A-7E). Consistently, the data showed that the inhibition of PTPMT1 disrupted mitochondrial function. The effects of PTPMT1 inhibition on glucose consumption and glucose transporter gene

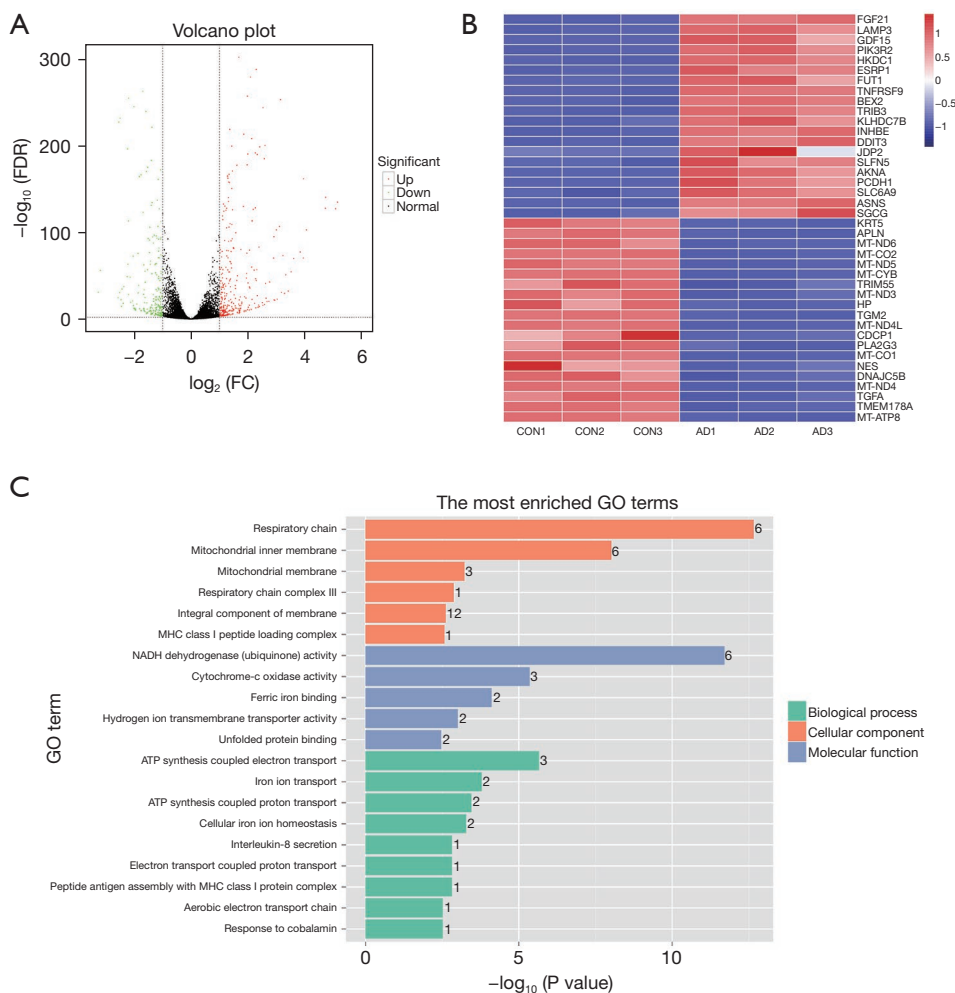


Figure 5 Transcriptome sequencing of the control and alexidine dihydrochloride groups. (A) Volcano plot of the differentially expressed genes. (B) Heat map of top 10 upregulated and downregulated genes between the two groups. (C) The most enriched GO terms in the alexidine dihydrochloride groups relative to the control groups. FDR, false discovery rate; FC, fold change; CON, control group; AD, alexidine dihydrochloride group; GO, Gene Ontology; MHC, major histocompatibility complex; NADH, nicotinamide adenine dinucleotide; ATP, adenosine triphosphate.

expression in the H69 cells were also examined. Glut-1 and Glut-3 expression was detected in the H69 cells transduced with PTPMT1 shRNA or the control vector. PTPMT1 knockdown significantly decreased Glut-1 and Glut-3 expression (Figure 7F-7G). To clarify the mechanisms by which PTPMT1 influenced glucose consumption, we further examined the effect of PTPMT1 knockdown on mitochondrial function in the H69 cells by JC-1 staining. PTPMT1-shRNA transduction significantly reduced the JC-1 level (Figure 7H). These results showed that PTPMT1 inhibition downregulated Glut1 and Glut3 expression, and disturbed mitochondrial function.

Discussion

The development of therapies with specific molecular targets has significantly improved the survival of cancer patients (27). However, the development of such targeted therapies relies on the identification of novel targets forms. Mitochondria function as the “powerhouse” of the cell, generating ATP through oxidative phosphorylation. Aberrant metabolism reprogramming is considered a biological characteristics of tumor cells (28). Targeting mitochondrial metabolism represents a novel therapeutic approach for cancer therapy (29). Mitochondrial

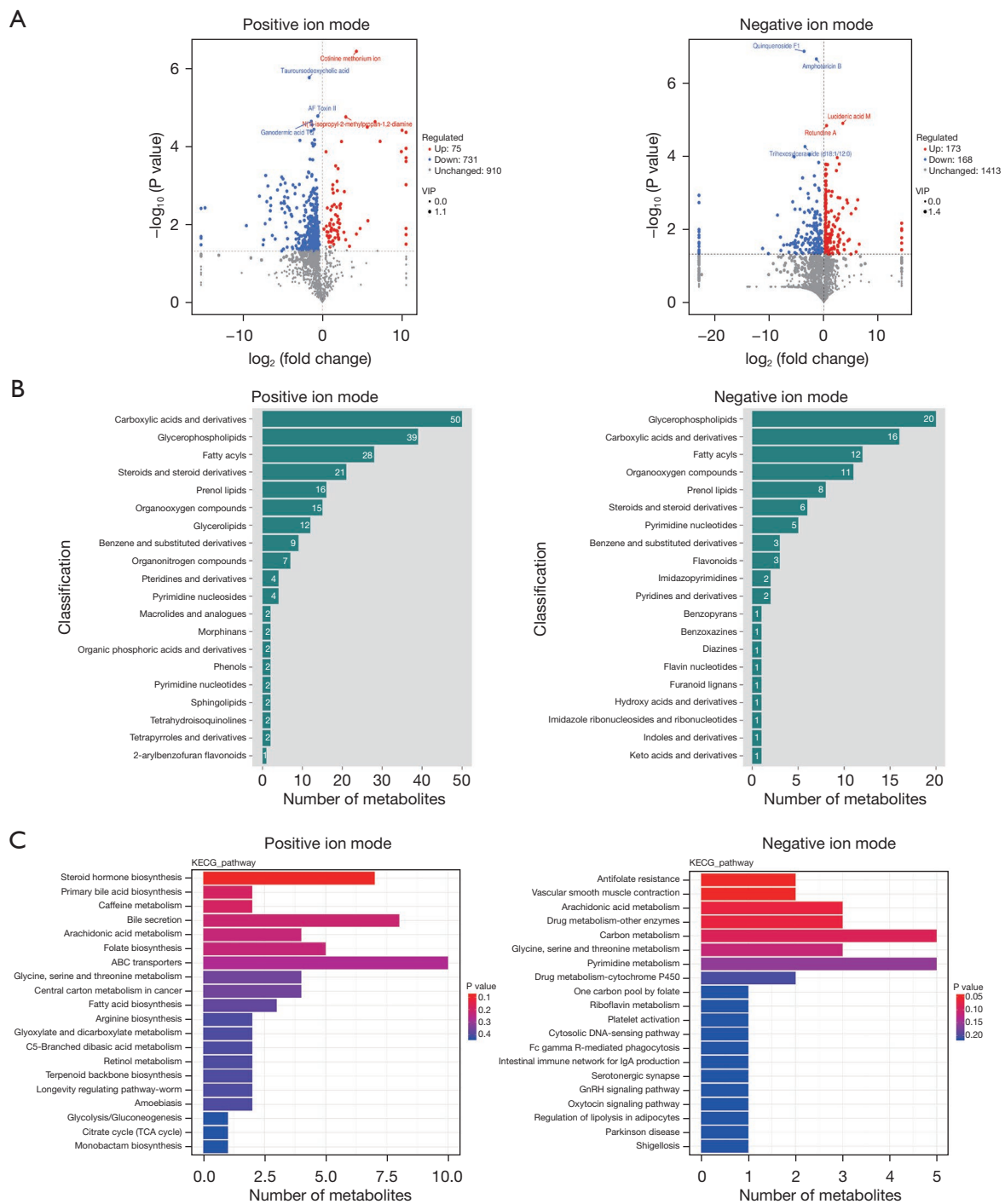


Figure 6 Untargeted metabolomics of the control and alexidine dihydrochloride groups. (A) Volcano plots of the differential metabolites in the positive and negative ion modes. (B) The classification of the differential metabolites in the positive and negative ion modes. (C) The KEGG pathway analysis of the differential metabolites in positive and negative ion modes. KEGG, Kyoto Encyclopedia of Genes and Genomes; VIP, Variable Importance for the Projection; ABC, ATP-binding cassette; TCA, tricarboxylic acid cycle.

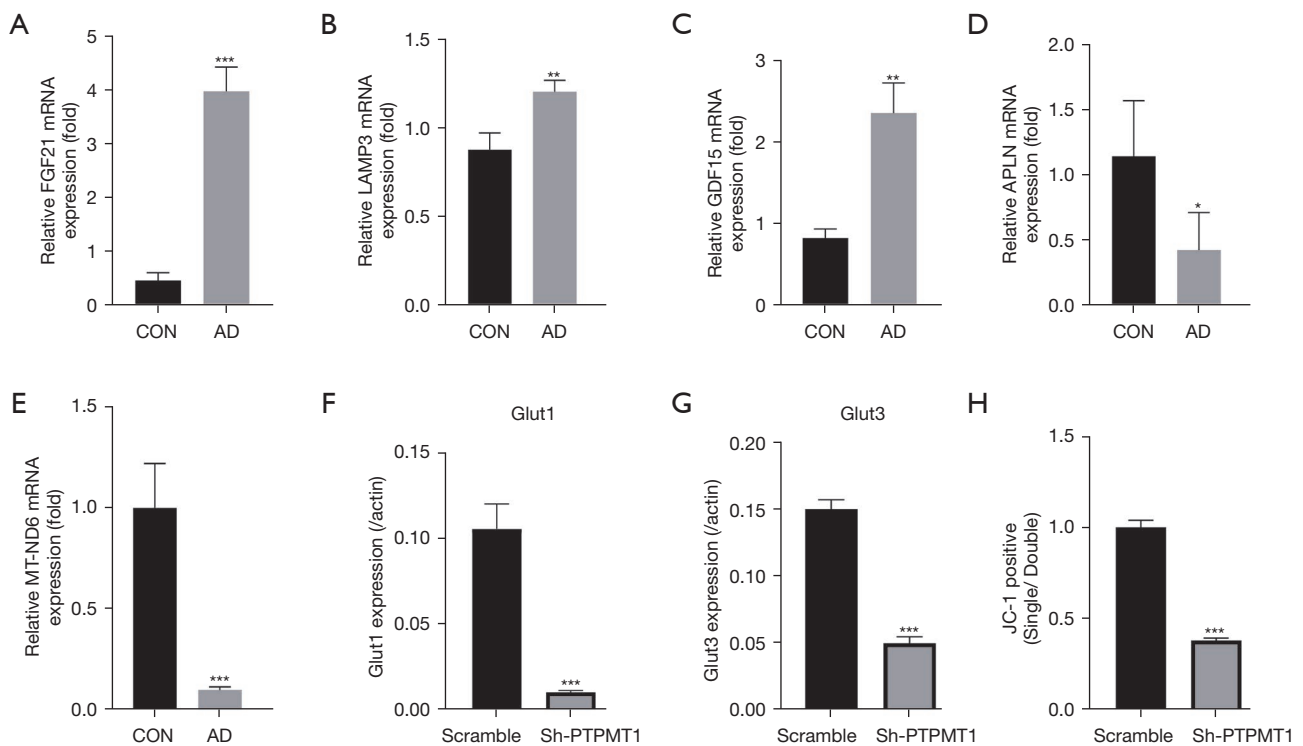


Figure 7 PTPMT1 inhibition reduces Glut expression. (A-E) The qRT-PCR analysis of the transcriptome differentially sequenced genes in H69 cells. *, $P < 0.05$; **, $P < 0.01$; ***, $P < 0.001$, AD 5 μM vs. control (DMSO). (F,G) The H69 cells were transduced with PTPMT1 shRNA. The expression of Glut1 and Glut3 was determined by qRT-PCR. ***, $P < 0.001$, sh-PTPMT1 vs. scramble (control). (H) The H69 cells were transduced with PTPMT1-shRNA or control vectors, and stained with JC-1 dye, and the ratio of the average fluorescence intensity of red/green was determined by flow cytometry. ***, $P < 0.001$, sh-PTPMT1 vs. scramble (control). PTPMT1, protein tyrosine phosphatase mitochondrial 1; qRT-PCR, quantitative real-time polymerase chain reaction; shRNA, short-hairpin RNA; DMSO, dimethylsulfoxide; AD, alexidine dihydrochloride; mRNA, messenger RNA.

phosphatases that regulate protein dephosphorylation and calibrate mitochondrial activities play an important role in mitochondrial metabolism (30). PTPMT1 is a critical mitochondrial phosphatase anchored in the mitochondrial inner member. PTPMT1 has been approved to regulate mitochondrial respiration, structure, and cardiolipin biosynthesis (31). PTPMT1 deletion impairs mitochondrial energy source selection, which is crucial for CD8⁺ T immune cell response (19). It calibrates mitochondrial activities and influences the fate of cells in various cell types (22,32,33). In a recent study, we showed that PTPMT1 modulates mitochondrial function via the SLC25A6-NDUFS2 axis in pancreatic ductal adenocarcinoma (34). In the present study, using immunochemistry staining, we showed that PTPMT1 is highly expressed in SCLC tissues compared with adjacent normal tissues. Moreover, a comprehensive TCGA analysis revealed that PTPMT1

overexpression was associated with a lower survival rate in patients with lung cancer. These results suggest that PTPMT1 contributes to tumor progression in SCLC.

PTPMT1 dysregulation is linked to aberrant mitochondrial metabolism in tumor cells. Our functional studies have shown that PTPMT1 plays essential roles in the proliferation and survival of SCLC cells. In this study, PTPMT1 expression was significantly silenced in the H69 and A549 cells following transduction with lentivirus-mediated shRNA. Cell activity was also significantly inhibited by the specific inhibitor alexidine dihydrochloride (35). Several consistent phenotypes, including a lower proliferation rate, reduced colony forming ability, and increased apoptosis were observed in the PTPMT1-shRNA-transduced H69 and A549 cells, and alexidine dihydrochloride-treated cells. These results show that the downregulation of the mitochondrial phosphatase PTPMT1

promoted cell death and reduced proliferation in SCLC cells.

The mechanisms of several types of regulated cell death, such as apoptosis, necrosis, and ferroptosis, have been well elucidated. The treatment of H69 and A549 cells with the PTPMT1 inhibitor alexidine dihydrochloride resulted in significant apoptosis. Recent research has focused on ferroptosis, another type of cell death, which is iron-dependent and differs from traditional regulated cell death, such as apoptosis, necrosis, and pyroptosis (36-38). We examined whether ferroptosis was involved in cell death induced by the inhibition of PTPMT1. Research has shown that Fer-1, a specific ferroptosis inhibitor, significantly attenuates erastin-induced cell death (39). However, Fer-1 does not reverse PTPMT1 inhibition-induced cell death. PTPMT1 protects human cells from erastin-induced ferroptosis in pancreatic cancer, but their anti-ferroptosis roles were not found to be involved in this process in lung cancer cells (33).

A transcriptome analysis was performed to explore the molecular mechanisms of PTPMT1. Significant changes were observed in the transcriptomes in the PTPMT1-inhibited cells. The dysregulated genes in the alexidine dihydrochloride-treated cells included *FGF21*, *LAMP3*, *GDF15*, *APLN*, *MT-ND6*, etc. Based on the GO and KEGG pathway analyses, these genes were involved in respiratory chain protein, mitochondria inner membrane, ATP synthesis coupled electron transport, and NADH dehydrogenase activity. Further, PTPMT1 inhibition disrupted mitochondrial metabolism, which led to cell apoptosis and growth arrest. Through untargeted metabolomics, the alexidine dihydrochloride treatment caused changes in several metabolites and their related metabolic pathways in the H69 cells.

Aberrant metabolic perturbation, such as cytosolic aerobic glycolysis, enables tumor cells to actively proliferate and enhances their survival. A previous study of leukemia cells showed that PTPMT1 appears to regulate glycolysis metabolism through glucose transporters (40). We found that PTPMT1 knockdown also downregulated the glucose transporters Glut1 and Glut3 in the SCLC cells. Further, JC-1 staining showed that PTPMT1 knockdown attenuated mitochondrial function. These results suggest that the inhibition of PTPMT1 influences Glut expression and disturbs mitochondrial function in SCLC cells.

PTPMT1 potentially may be considered as an early diagnostic and prognostic marker for SCLC. At present, challenges that need to be solved urgently is the way of drug delivery and its targeted therapy. Our future directions will

be the effects of PTPMT1 in SCLC *in vivo*. By improving the targeting ability of PTPMT1 inhibitors to better act on cancer cells through using nano vesicles or extracellular vesicles and so on, which may improve the inhibitory effect of PTPMT1 (41). Further research is needed to discover the mechanism of mitochondrial function in the process of tumorigenesis for better utilization in the clinic.

Conclusions

This study showed that PTPMT1 is highly expressed in SCLC tissues. Further, we found that PTPMT1 inhibition induces the apoptosis and growth arrest of human SCLC cells by disrupting mitochondrial and glucose metabolism. Thus, these results suggest that targeting PTPMT1 might provide a novel therapeutic approach to the treatment of SCLC.

Acknowledgments

We would like to thank Qinghai Provincial People's Hospital for supplying SCLC samples.

Funding: This work was supported by funding from the National Natural Science Foundation of China (Nos. 82102747 and 82160489), the Hebei Province Innovation Enhancement Project (No. 22567663H), and the Natural Science Foundation of Qinghai Province (No. 2022-ZJ-733).

Footnote

Reporting Checklist: The authors have completed the MDAR reporting checklist. Available at <https://tcr.amegroups.com/article/view/10.21037/tcr-2024-2379/rc>

Data Sharing Statement: Available at <https://tcr.amegroups.com/article/view/10.21037/tcr-2024-2379/dss>

Peer Review File: Available at <https://tcr.amegroups.com/article/view/10.21037/tcr-2024-2379/prf>

Conflicts of Interest: All authors have completed the ICMJE uniform disclosure form (available at <https://tcr.amegroups.com/article/view/10.21037/tcr-2024-2379/coif>). The authors have no conflicts of interest to declare.

Ethical Statement: The authors are accountable for all aspects of the work in ensuring that questions related to the accuracy or integrity of any part of the work

are appropriately investigated and resolved. The study was conducted in accordance with the Declaration of Helsinki (as revised in 2013). The study was authorized by Human Genetic Resource Administration of China (No. 2021SLCJ2445) and approved by ethics board of Qinghai Provincial People's Hospital (No. 2021-14-1). Informed consent was taken from all the patients.

Open Access Statement: This is an Open Access article distributed in accordance with the Creative Commons Attribution-NonCommercial-NoDerivs 4.0 International License (CC BY-NC-ND 4.0), which permits the non-commercial replication and distribution of the article with the strict proviso that no changes or edits are made and the original work is properly cited (including links to both the formal publication through the relevant DOI and the license). See: <https://creativecommons.org/licenses/by-nc-nd/4.0/>.

References

- Denning DW. Global incidence and mortality of severe fungal disease. *Lancet Infect Dis* 2024;24:e428-38.
- Srivastava R, Lebowicz Y, Jamil MO. Targeted agents in the management of small cell lung cancer - present and future. *Drugs Today (Barc)* 2018;54:479-88.
- Kalemkerian GP. Small Cell Lung Cancer. *Semin Respir Crit Care Med* 2016;37:783-96.
- Jin Y, Chen Y, Qin Z, et al. Understanding SCLC heterogeneity and plasticity in cancer metastasis and chemotherapy resistance. *Acta Biochim Biophys Sin (Shanghai)* 2023;55:948-55.
- Cao S, Wang Y, Zhou Y, et al. A Novel Therapeutic Target for Small-Cell Lung Cancer: Tumor-Associated Repair-like Schwann Cells. *Cancers (Basel)* 2022;14:6132.
- Lu T, Yang X, Huang Y, et al. Trends in the incidence, treatment, and survival of patients with lung cancer in the last four decades. *Cancer Manag Res* 2019;11:943-53.
- Li Y, Hu S, Xie J, et al. Effects of surgery on survival of elderly patients with stage I small-cell lung cancer: analysis of the SEER database. *J Cancer Res Clin Oncol* 2019;145:2397-404.
- Hamilton G, Hochmair MJ, Stickler S. Overcoming resistance in small-cell lung cancer. *Expert Rev Respir Med* 2024;18:569-80.
- Wang Q, Tan LM. Advances in the role of circulating tumor cell heterogeneity in metastatic small cell lung cancer. *Cancer Innov* 2023;3:e98.
- Porporato PE, Filigheddu N, Pedro JMB, et al. Mitochondrial metabolism and cancer. *Cell Res* 2018;28:265-80.
- Vasan K, Werner M, Chandel NS. Mitochondrial Metabolism as a Target for Cancer Therapy. *Cell Metab* 2020;32:341-52.
- Huang M, Myers CR, Wang Y, et al. Mitochondria as a Novel Target for Cancer Chemoprevention: Emergence of Mitochondrial-targeting Agents. *Cancer Prev Res (Phila)* 2021;14:285-306.
- Xiao J, Engel JL, Zhang J, et al. Structural and functional analysis of PTPMT1, a phosphatase required for cardiolipin synthesis. *Proc Natl Acad Sci U S A* 2011;108:11860-5.
- Pagliarini DJ, Worby CA, Dixon JE. A PTEN-like phosphatase with a novel substrate specificity. *J Biol Chem* 2004;279:38590-6.
- Nath AK, Ryu JH, Jin YN, et al. PTPMT1 Inhibition Lowers Glucose through Succinate Dehydrogenase Phosphorylation. *Cell Rep* 2015;10:694-701.
- Zheng H, Yu WM, Shen J, et al. Mitochondrial oxidation of the carbohydrate fuel is required for neural precursor/stem cell function and postnatal cerebellar development. *Sci Adv* 2018;4:eat2681.
- Yu WM, Liu X, Shen J, et al. Metabolic regulation by the mitochondrial phosphatase PTPMT1 is required for hematopoietic stem cell differentiation. *Cell Stem Cell* 2013;12:62-74.
- Zhang CC, Sadek HA. Hypoxia and metabolic properties of hematopoietic stem cells. *Antioxid Redox Signal* 2014;20:1891-901.
- Chen C, Zheng H, Horwitz EM, et al. Mitochondrial metabolic flexibility is critical for CD8(+) T cell antitumor immunity. *Sci Adv* 2023;9:eadf9522.
- Chen HX, Ma YZ, Xie PP, et al. Micropeptide MPM regulates cardiomyocyte proliferation and heart growth via the AKT pathway. *Biochim Biophys Acta Mol Cell Res* 2024;1871:119820.
- Sheng J, Zhao Q, Zhao J, et al. SRSF1 modulates PTPMT1 alternative splicing to regulate lung cancer cell radioresistance. *EBioMedicine* 2018;38:113-26.
- Niemi NM, Lanning NJ, Westrate LM, et al. Downregulation of the mitochondrial phosphatase PTPMT1 is sufficient to promote cancer cell death. *PLoS One* 2013;8:e53803.
- Bao MH, Yang C, Tse AP, et al. Genome-wide CRISPR-Cas9 knockout library screening identified PTPMT1 in cardiolipin synthesis is crucial to survival in hypoxia in liver cancer. *Cell Rep* 2021;34:108676.

24. Weisberg SP, Smith-Raska MR, Esquelin JM, et al. ZFX controls propagation and prevents differentiation of acute T-lymphoblastic and myeloid leukemia. *Cell Rep* 2014;6:528-40.
25. Xu QQ, Xiao FJ, Sun HY, et al. Ptpmt1 induced by HIF-2 α regulates the proliferation and glucose metabolism in erythroleukemia cells. *Biochem Biophys Res Commun* 2016;471:459-65.
26. Gao CC, Xu QQ, Xiao FJ, et al. NUDT21 suppresses the growth of small cell lung cancer by modulating GLS1 splicing. *Biochem Biophys Res Commun* 2020;526:431-8.
27. Herbst RS, Morgensztern D, Boshoff C. The biology and management of non-small cell lung cancer. *Nature* 2018;553:446-54.
28. Rodrigues T, Ferraz LS. Therapeutic potential of targeting mitochondrial dynamics in cancer. *Biochem Pharmacol* 2020;182:114282.
29. Sotgia F, Ozsvari B, Fiorillo M, et al. A mitochondrial based oncology platform for targeting cancer stem cells (CSCs): MITO-ONC-RX. *Cell Cycle* 2018;17:2091-100.
30. Srinivasan S, Guha M, Kashina A, et al. Mitochondrial dysfunction and mitochondrial dynamics-The cancer connection. *Biochim Biophys Acta Bioenerg* 2017;1858:602-14.
31. Zhang J, Guan Z, Murphy AN, et al. Mitochondrial phosphatase PTPMT1 is essential for cardiolipin biosynthesis. *Cell Metab* 2011;13:690-700.
32. Chen Z, Zhu S, Wang H, et al. PTPMT1 Is Required for Embryonic Cardiac Cardiolipin Biosynthesis to Regulate Mitochondrial Morphogenesis and Heart Development. *Circulation* 2021;144:403-6.
33. Huang XD, Xiao FJ, Guo YT, et al. Protein tyrosine phosphatase 1 protects human pancreatic cancer from erastin-induced ferroptosis. *Asian J Surg* 2022;45:2214-23.
34. Ding PP, Huang XD, Shen L, et al. PTPMT1 regulates mitochondrial death through the SLC25A6-NDUFS2 axis in pancreatic cancer cells. *Am J Cancer Res* 2023;13:992-1003.
35. Doughty-Shenton D, Joseph JD, Zhang J, et al. Pharmacological targeting of the mitochondrial phosphatase PTPMT1. *J Pharmacol Exp Ther* 2010;333:584-92.
36. Latunde-Dada GO. Ferroptosis: Role of lipid peroxidation, iron and ferritinophagy. *Biochim Biophys Acta Gen Subj* 2017;1861:1893-900.
37. Dixon SJ, Lemberg KM, Lamprecht MR, et al. Ferroptosis: an iron-dependent form of nonapoptotic cell death. *Cell* 2012;149:1060-72.
38. Tonnus W, Meyer C, Paliege A, et al. The pathological features of regulated necrosis. *J Pathol* 2019;247:697-707.
39. Xiao FJ, Zhang D, Wu Y, et al. miRNA-17-92 protects endothelial cells from erastin-induced ferroptosis through targeting the A20-ACSL4 axis. *Biochem Biophys Res Commun* 2019;515:448-54.
40. Xu QQ, Xiao FJ, Sun HY, et al. Ptpmt1 induced by HIF-2 α regulates the proliferation and glucose metabolism in erythroleukemia cells. *Biochem Biophys Res Commun* 2016;471:459-65.
41. Kumar MA, Baba SK, Sadida HQ, et al. Extracellular vesicles as tools and targets in therapy for diseases. *Signal Transduct Target Ther* 2024;9:27.

Cite this article as: Liu X, Sun Y, Gao C, Sun H, Tian F, Xiao F, Xu Q. PTPMT1 inhibition induces apoptosis and growth arrest of human SCLC cells by disrupting mitochondrial metabolism. *Transl Cancer Res* 2024;13(12):6956-6969. doi: 10.21037/tcr-2024-2379